EUROPEAN COMMISSION
Community research

BELBaR

(Contract Number: 295487)

DELIVERABLE (D-N°:D4.9)

Rheology of attractive and repulsive montmorillonite/bentonite gels

Authors:
Magnus Hedström, Ulf Nilsson Clay Technology AB
Rasmus Eriksson, B+Tech Oy

Reporting period: **01/03/12 – 29/02/16**

Date of issue of this report: **31/05/15**

Start date of project: **01/03/12** Duration: 48 Months

Project co-funded by the European Commission under the Seventh Euratom Framework Programme for Nuclear Research &Training Activities (2007-2011)

Dissemination Level		
PU	Public	PU
RE	Restricted to a group specified by the partners of the BELBaR project	
CO	Confidential, only for partners of the BELBaR project	

EURATOM

DISTRIBUTION LIST

Name	Number of copies	Comments
Christophe Davies (EC) BELBaR participants		

Introduction

Understanding rheological properties of montmorillonite/bentonite is important for assessing the fate of clay in a geological repository for spent nuclear fuel, especially under dilute groundwater conditions. Smectite clays such as montmorillonite have complicated phase diagrams with several arrested states, especially different kinds of repulsive gels as well as various sol states. To simplify the picture somewhat, we only consider attractive and repulsive gels, and sol. The attractive gel consists of a volume-spanning network of connected clay particles that is formed when the clay particle concentration is above the percolation threshold and the salinity is higher than a critical concentration value. The attractive gel has yield strength and the attractive particle-particle forces withstands the osmotic pressure so the gel does not expand even in contact with excess electrolyte. Sols are by definition liquid colloidal systems. In very dilute sols, the clay particles can be treated as non-interacting, and sometimes this system is referred to as a gas or gaseous sol. But the phase as a whole is liquid since the clay particles are suspended in an aqueous solution. At higher clay concentration (volume fraction) the clay particle may interact, but the phase is still liquid, i.e. a sol. At sufficiently high clay concentration, the osmotic repulsion (overlapping double layer) forces may dominate giving the system solid-like properties. This is conventionally termed repulsive gel, albeit direct particle-particle contact may be absent.

Erosion studies using artificial fracture systems have shown that when an attractive gel is formed at the swelling front, the penetration of the clay into the fracture is limited and erosion is below detection limit. Thus erosion of bentonite in a repository is only expected when conditions are such that a sol can be formed. Yield stress measurements on attractive gels reported here (contribution by Clay Technology AB) confirms that attractive gels are expected to withstand the shear forces from the flowing water.

Similarly, the work on repulsive gels and sols in this report (contribution by B+Tech Oy) shows that mechanical erosion of the repulsive gel at the gel-sol interface is highly unlikely. Thus, erosion under dilute water conditions is a matter of repulsive gel to sol transition and the removal rate of the sol.

The present work on attractive gels is performed using montmorillonite from the Indian bentonite Asha 505.

The work on repulsive gels and sols in this study was conducted using Wyoming montmorillonite extracted from MX-80 bentonite.

Results from Clay Technology AB

Phenomenological description of attractive montmorillonite gels:

An attractive clay gel is defined by a volume-spanning network of connected clay platelets through attractive forces. The network forces are strong enough to withstand the osmotic repulsion. Thus an attractive gel does not expand in contact with excess electrolyte. Figure 1 shows the behavior of a suspension at 20g/l of Ku-Na montmorillonite (Na^+ homo-ionized montmorillonite from Asha 505 bentonite, Kutch district, India) in contact with air (left) and in contact with excess electrolyte (right), respectively. The NaCl concentration in the suspension and in the excess electrolyte was the same: 20 mM. In contact with air the suspension appears liquid-like, while in contact with excess electrolyte the gel characteristics become evident. These seemingly contradicting behaviors of the Ku-Na suspension occur in the same sample and depends only on the boundary between the clay-rich phase and the surrounding. The gel-like property transpires immediately after the interface with air is removed by adding extra electrolyte. As it is unlikely that the addition of further electrolyte would instantly cause network bond formation, we must conclude that the volume-spanning network of clay platelets was already present. The clay-particle network has low mobility while the electrolyte move through the system as a liquid. Thus when the gel borders air, capillary forces emerge when the vial is tilted and the electrolyte leaves the network structure. Obviously the forces connecting the clay particles cannot withstand the capillary forces. This causes the gel to appear as a liquid in the photo to the left in Figure 1. The physics is similar to the capillary induced deformation and collapse of flexible walls (Cambau et al., 2011; Tas et al., 2010). When the gel borders excess electrolyte, there are no capillary forces and the gel behavior is clearly manifested (Figure 1, right). In this study we will examine the shear stress as a function of strain to determine the yield stress of Asha 505 montmorillonite at NaCl concentrations above the critical coagulation concentration.

Homo-ionic Ku-Na montmorillonite forms attractive gels at NaCl concentrations as low as 4 mM, while at 3 mM we have never found any gel.

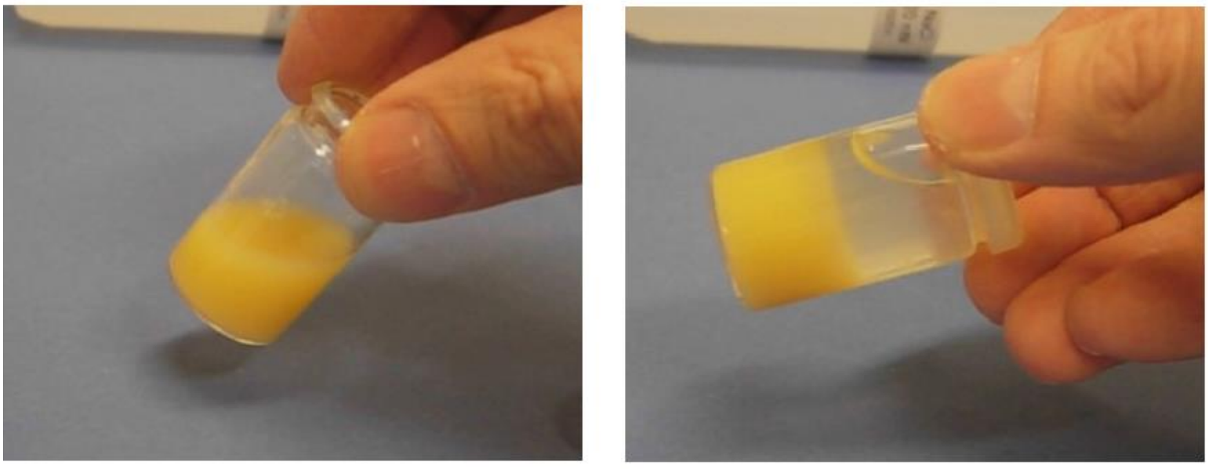

Figure 1. Ku-Na montmorillonite, 20g/l, in 20 mM NaCl. Left: Behavior of the suspension when the interface is air. Right: The same suspension with 6 ml 20 mM NaCl(aq) added on top of the suspension to give an interface to a liquid.

Material:

Raw (as received) Asha505 bentonite was dispersed in deionized (DI) water (10g/l) and sonicated for 15 minutes. Then the suspensions were left on magnetic stirrer overnight. The <2µm fraction, which essentially consists of montmorillonite, was extracted from the bentonite suspension using centrifugation. The suspension containing the <2µm fraction was placed in 60 °C oven until the water had evaporated (approximately 3 days). The oven-dried montmorillonite was subsequently milled to a fine powder. Note that the montmorillonite is not homo-ionized. A previous determination of exchangeable ions showed that the montmorillonite fraction of Asha 505 contains Mg^{2+} (28%), Ca^{2+} (31%), Na^{+} (40%), and K^{+} (1%) (Karnland et al., 2006). Since the origin of Asha bentonite is the Kutch district in India we hereafter refer to the montmorillonite (<2µm fraction) as Ku-mmt.

Sample preparation:

Stock dispersions (20g/l and 40g/l) of Ku-mmt were prepared by mixing the montmorillonite powder with DI water using magnetic stirrer. After ~20h the dispersions appeared homogeneous and smooth. After ~24h the dispersions were added to NaCl solutions. Each sample cup was filled with 15 ml of NaCl(aq) (double strength) and 15 ml of Ku-mmt stock dispersion was added. The sample was capped and vigorously shaken 50 (5 and 10 mM final ionic strength) or 100 times (50 and 100 mM final ionic strength) and left to rest (1 day or 1 week) before the rheology tests. After examining the yield-stress results from the first series of experiment, we decided to also perform tests on Ku-mmt in 20 mM NaCl(aq). Those samples were neither prepared from the same stock dispersion, nor by the same person.

Yield-stress measurements:

Yield stress was measured with rotating vane rheometry (Barnes and Nguyen, 2001) using a Brookfield DV II + Pro LV viscometer and the V-73 vane spindle. The vane was lowered into the clay sample and the measurement was started immediately. The yield-stress measurement was conducted at a low constant rotational rate of 0.05 rpm for 500-800 s. The yield stress is taken as the peak value in the stress-time curve (equivalent to stress-strain curve).

Results

Figure 2 display the appearance of a Ku-mmt gel after a yield stress measurement.

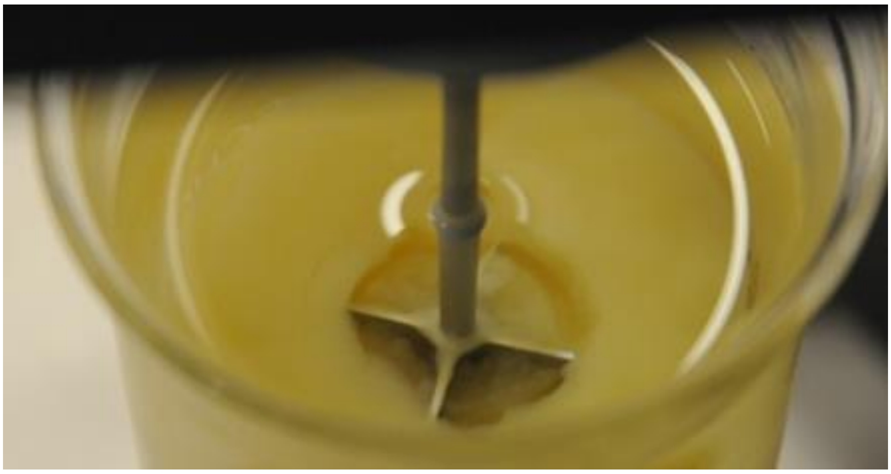

Figure 2. Ku-mmt, 20g/l in 20 mM NaCl(aq) after a yield stress measurement.

The vane spindle has clearly cut out a cylinder in the gel. The dimensions of the V-73 vane spindle are 25.35 mm in height and 12.67 mm in “diameter”. The remaining pattern is stable and the gel does not spontaneously reform on a “laboratory” timescale. This suggests that when the gel is broken, the clay particles at the gel surfaces arrange themselves into new local energy minima. Thus there is a barrier for the clay particles to reconnect with particles on the neighboring surface. Figure 2 represents yet another strong evidence that these systems really are attractive gels. In Figure 2 the gel is covered with excess electrolyte to avoid capillary-induced collapse at the top surface, which would ruin the pedagogical point of the photo. In the actual measurements behind the data in this report, no excess electrolyte were added. Also the spindle was “properly” immersed into the gel up mark at the middle of the shaft (the mark is visible at the water surface in Figure 2).

All measurements in this study were made in triplicates, except for the non-gelled samples without any added NaCl (duplicates). The results for Ku-mmt at 10 g/l and 24 h rest time are shown in Figure 3. With no added salt, the shear stress was constantly below measurement threshold. The samples prepared in NaCl(aq) had all developed yield strength. Furthermore, the agreement among the triplicate samples was very good. The effect of salinity on the maximum stress (here chosen as the yield stress) is particularly high at the lower concentrations: the value of ~1.5 Pa at 10 mM is more than three times larger than the value at 5 mM, ~0.5 Pa. The yield stress curves seem to converge at the two highest NaCl concentrations. The increase in NaCl concentration from 10 to 50 mM gave an increase in yield stress from ~1.5 to ~2.5 Pa (see also Table 1). There is also a pronounced increase in shear modulus with increasing NaCl concentration, in line with the increase in yield stress.

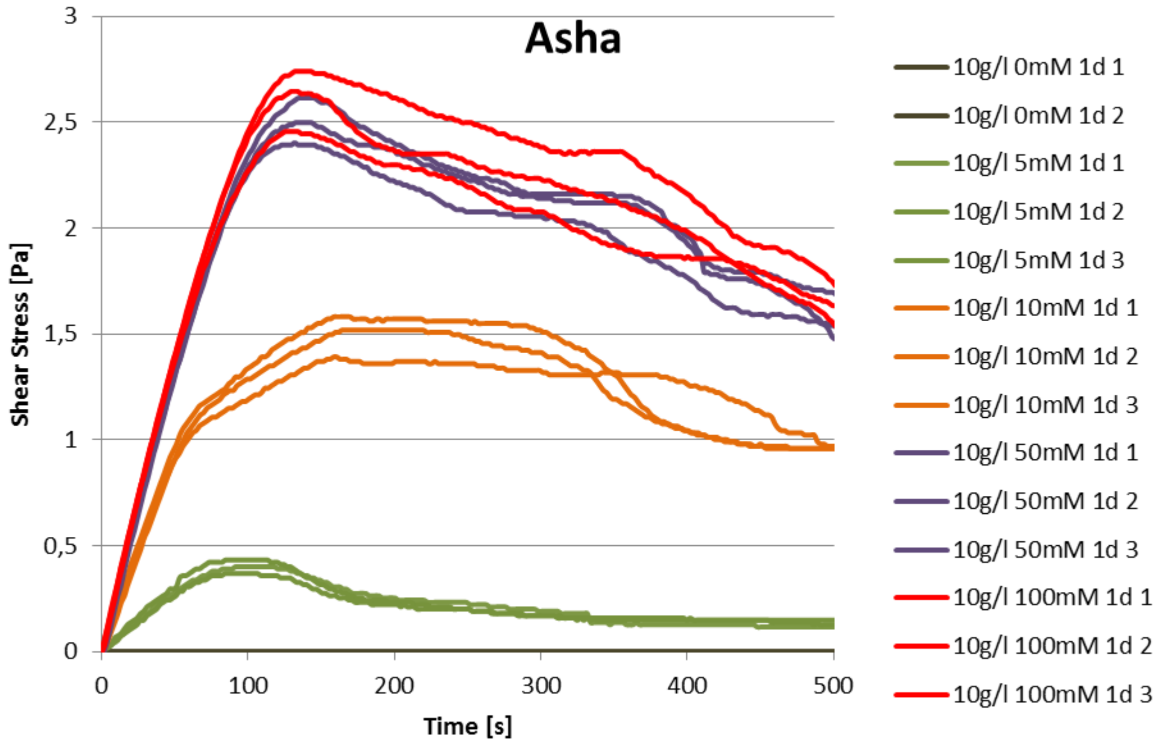

Figure 3. Shear stress vs time for Ku-mmt at a concentration of 10g/l and different NaCl concentrations 24 hours after preparation. Note that without extra NaCl, denoted 0mM in the legend, the suspension has no yield stress at all, and the two curves coincide with the x-axis.

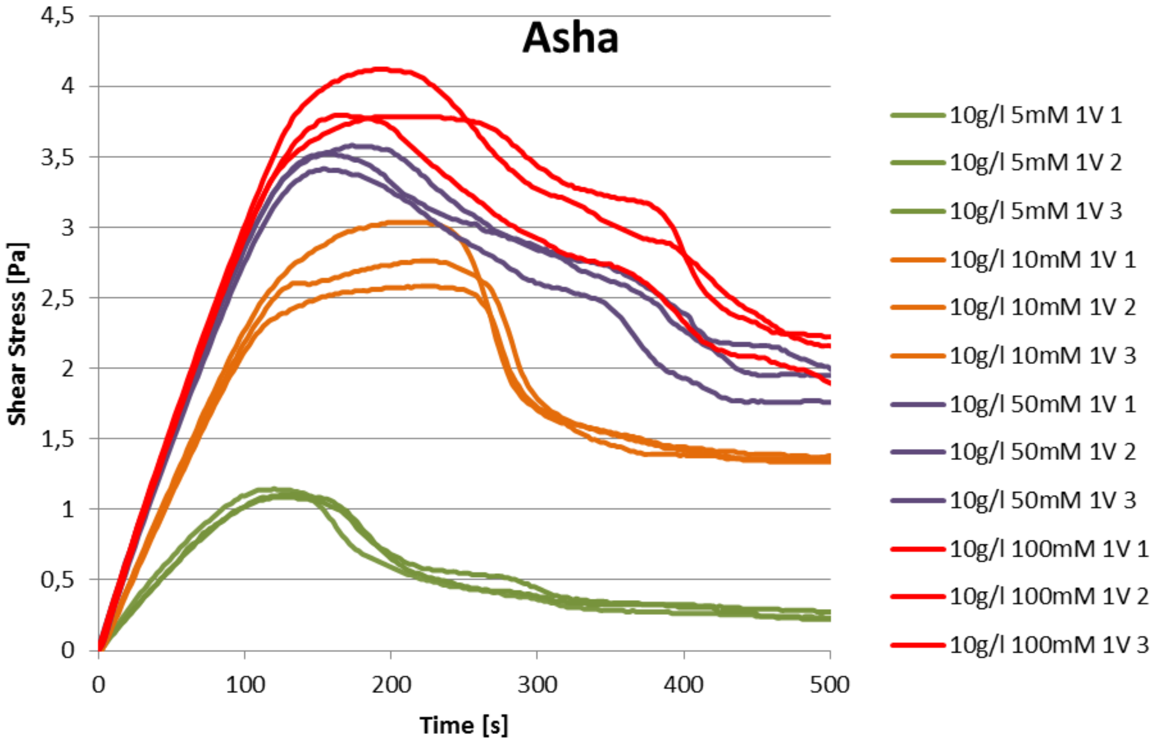

Figure 4. Shear stress vs time for Ku-mmt at a concentration of 10g/l and different NaCl concentrations 1 week after preparation.

It is well known that aging can have profound effect on rheological properties. This is illustrated by comparing Figure 3 and Figure 4. Letting clay samples rest for a week gives a significant increase in both shear modulus and yield stress. The effect is larger for gels formed at lower concentrations, which is logical: weaker bonds need less thermal agitation to explore configuration space, thus the effect of optimizing the overall gel structure is detectable on a shorter timescale.

Increasing the solids content has an even larger effect on yield stress than aging. Figure 5 shows the shear stress curves obtained after 24 h for Ku-mmt at a concentration of 20g/l. Again, without the addition of NaCl the shear stress was below detection. The largest effect of increasing clay concentration is seen for the samples at 5 mM, where the average yield stress has increased to 4.4 Pa, a factor of 11 compared to the value at 10 g/l (Figure 3 and Table 1). At the other NaCl concentrations the increase in yield stress is about a factor of 3.5 which is still significant and not far from the “anticipated” value of 2^2=4 (Russel et al., 1992). In Figure 5 we also show results obtained at 20 mM NaCl. These samples appear to have higher yield stress than the 50 mM samples. This non-trivial variation of yield with salinity has also been seen in other types of experiments (Hansen and Hedström, 2015) and is a signature of the Coulombic attraction between the positive edges and the negative faces of the clay particles. It should be noted however, that these samples were prepared at a later occasion using a different Ku-mmt stock solution. One week aging caused the 100 mM samples to have yield stress above the measuring range so tests were performed by inserting the vane halfway. Unfortunately that did not give reliable values as can be seen from the scatter in Figure 6. The 5 mM samples showed similar increase in yield stress upon aging as for the 10g/l samples. In fact there are 5 mM curves in Figure 6 showing higher yield stress than some of the

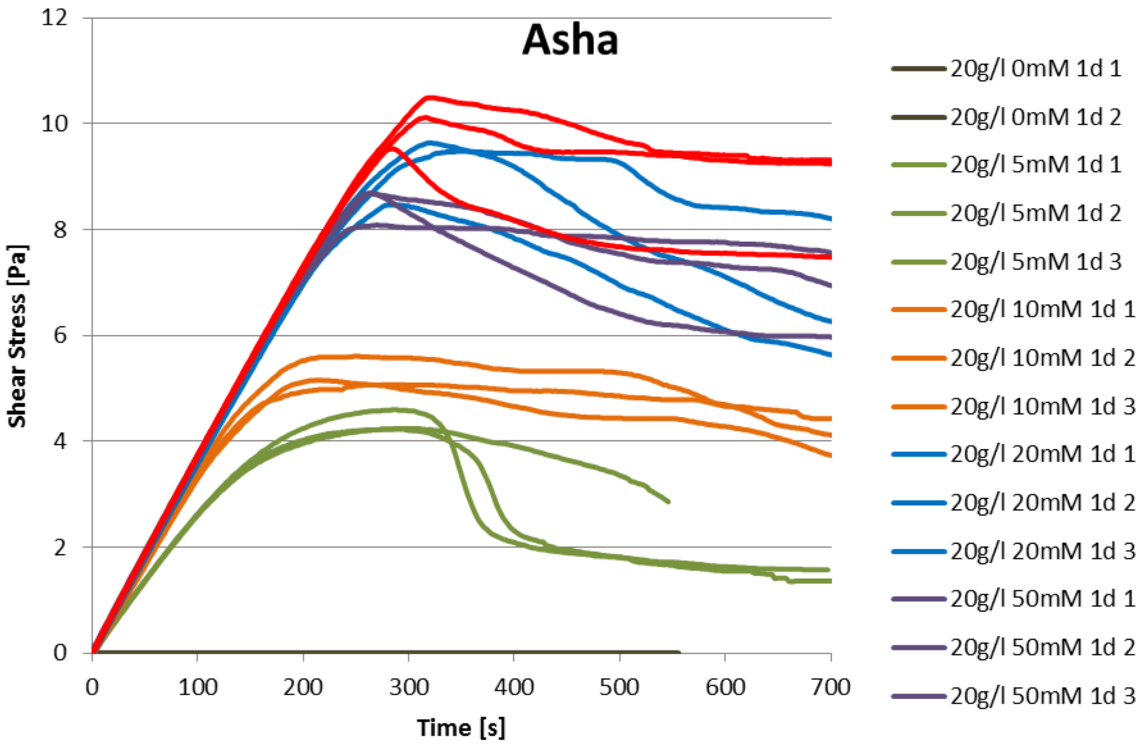

Figure 5. Shear stress vs time for Ku-mmt at a concentration of 20g/l and different NaCl concentrations 24 hours after preparation. Note that without extra NaCl, denoted 0mM in the legend, the suspension has no yield stress at all, and the two curves coincide with the x-axis.

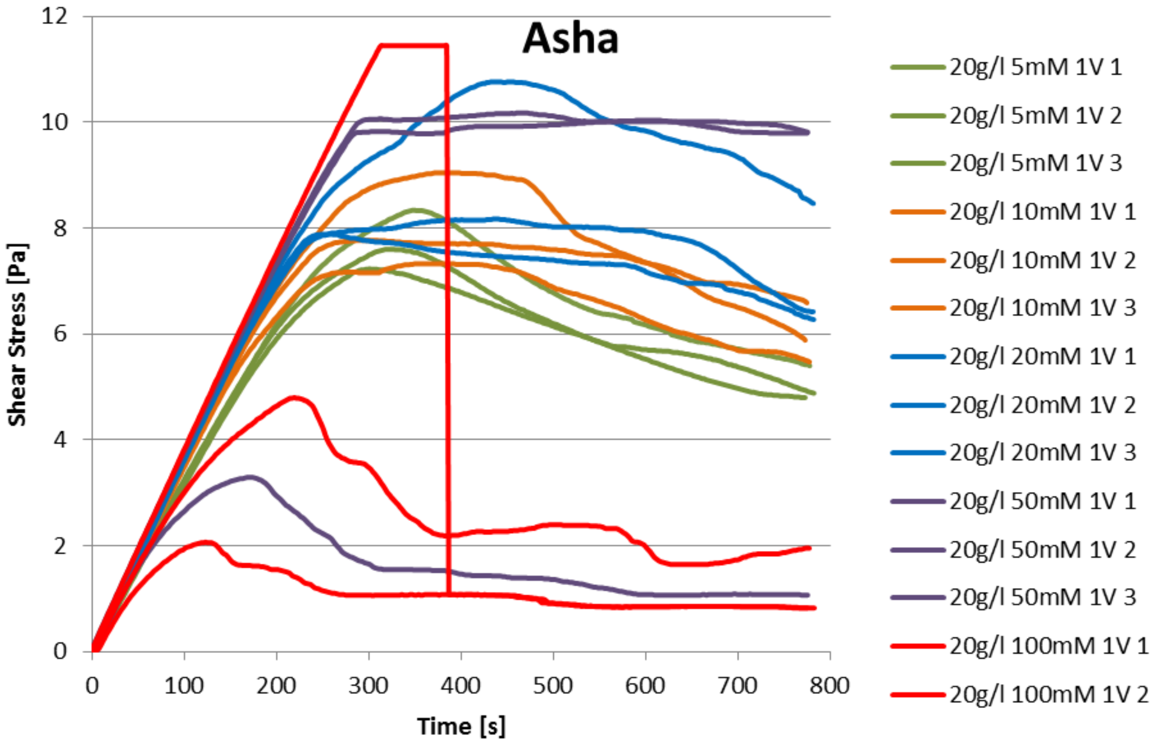

Figure 6. Shear stress vs time for Ku-mmt at a concentration of 20g/l and different NaCl concentrations 1 week after preparation. Note that for the 100 mM sample the stress is higher than instrument measuring range. Therefore tests were done by inserting the vane spindle only halfway into the gel (the lowest two 100 mM and lowest 50 mM curves).

	Average maximum yield stress (Pa)			
C_{mmt} **[NaCl]**	10g/l, 24 h	10g/l, 1 week	20g/l, 24 h	20g/l, 1 week
5 mM	0.4	1.1	4.4	7.7
10 mM	1.5	2.8	5.3	8.0
20 mM	-	-	9.2	8.9
50 mM	2.5	3.5	8.5	-
100 mM	2.6	3.9	10.0	-

Table 1. Average yield stress from the rheological measurements in Figure 3 to Figure 6.

measurements on 10 and 20 mM samples. Possibly there are artefacts making the aged samples at higher salinity to show too low shear stress. Further experiments are needed to settle this issue. It was noticed during preparation that air bubbles tended to be trapped inside the stronger gels. For the next series of experiments even more efforts will be made to increase the homogeneity of the gels. In order to also measure higher stresses a smaller vane spindle has been obtained.

Summary and considerations for geological disposal

Gel formation is the only bentonite-specific mechanism that can prevent erosion of clay at a transmissive fracture. The present tests show strong sensitivity to the salinity of the external water. For Ku-mmt a NaCl concentration of ~5 mM is needed to form a gel. However, even at such low concentration the present tests show that the yield stress is significant. In fact, all tested gels have yield stresses several orders of magnitude higher than the anticipated drag force of the flowing water in a repository (Eriksson and Schatz, 2015). The yield stress also shows strong dependence on clay concentration. This dependence is even stronger than that on salinity. The highest clay concentration in this study is 20g/l, but at a repository one may expect higher clay concentrations at the repulsive-attractive gel border adjacent to the ground water. In the present study we also reconfirm the effect of aging. One week of resting produce significantly stronger gels than those tested after 24 hours. At installation of the buffer bentonite in a future repository, the ground water conditions are such that an attractive gel will be formed at the swelling front and strongly limit penetration of bentonite into water-bearing fractures. These conditions will prevail at least until the next glaciation. Thus the attractive gel, most probably will attain its maximum strength.

References:

Barnes, H.A., Nguyen, Q.D., 2001. Rotating vane rheometry — a review. J. Non-Newton. Fluid Mech. 98, 1–14. doi:10.1016/S0377-0257(01)00095-7
Cambau, T., Bico, J., Reyssat, E., 2011. Capillary rise between flexible walls. EPL Europhys. Lett. 96, 24001. doi:10.1209/0295-5075/96/24001
Eriksson, R., Schatz, T., 2015. Rheological properties of clay material at the solid/solution interface formed under quasi-free swelling conditions. Appl. Clay Sci. 108, 12–18. doi:10.1016/j.clay.2015.02.018
Hansen, E., Hedström, M., 2015. Thermoreversible behaviour in smectite clay gel.
Karnland, O., Olsson, S., Nilsson, U., 2006. Mineralogy and sealing properties of various bentonites and smectite-rich clay material (Technical Report No. 06-30). SKB.
Russel, W.B., Saville, D.A., Schowalter, W.R., 1992. Colloidal Dispersions. Cambridge University Press.

Tas, N.R., Escalante, M., van Honschoten, J.W., Jansen, H.V., Elwenspoek, M., 2010. Capillary Negative Pressure Measured by Nanochannel Collapse. Langmuir 26, 1473–1476. doi:10.1021/la903649n

Results from B+Tech Oy

Introduction – Rheology

An external force applied on any liquid results in deformation and flow of the liquid. These processes are studied in rheology. All liquids exhibit a resistance to flow which is called the 'coefficient of viscosity', or simply just 'viscosity'. The higher the viscosity the higher the force that has to be applied onto a liquid to attain a certain flow velocity. Many liquids also display elastic character, meaning that an energy input in the form of a strain deformation is stored elastically in the structure and upon removal of the strain it reverts back to its original state, i.e. analogous to a spring.

Basic definitions

Viscosity is the most commonly used parameter to describe the rheological properties of a fluid. Two definitions exist for expressing viscosity, namely dynamic viscosity and kinematic viscosity of which the latter is simply the dynamic viscosity divided by the density of the fluid. The dynamic viscosity is often dependent on the current shear rate, and can vary considerably for a fluid as a function of shear rate. On the contrary, a fluid with constant viscosity as a function of shear rate is referred to as a Newtonian fluid. For many fluids, both behaviors are observed within certain shear rate ranges. Throughout this work, the word 'viscosity' refers to 'dynamic viscosity' unless otherwise stated in the text.

The setup for defining dynamic viscosity consists of two parallel plates separated by a distance *d* in between which the fluid is located (Fig. 1). When a force is applied on the upper plate it starts to move with a velocity *v*, creating a velocity gradient in the fluid between the upper plate and the stationary lower plate (Fig. 1). The force, *F*, per unit area required to move the upper plate (with an area *A* in contact with the fluid) to reach a certain velocity is called the *shear stress* ($\tau = F/A$) and depends on the viscosity of the fluid.

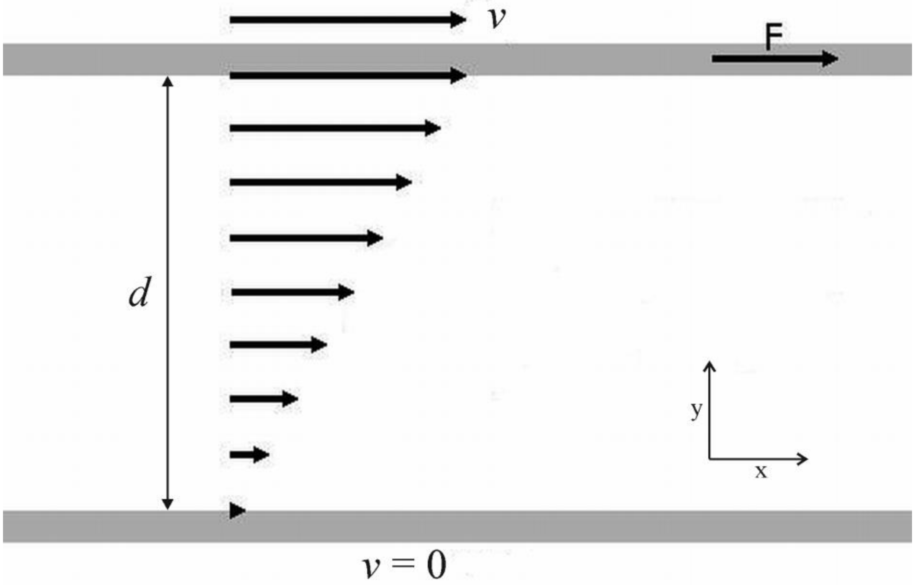

Figure 1. Schematic picture illustrating two parallel plates separated by a distance *d* with a liquid in between them. A force is applied on the upper plate (the lower plate is stationary) which starts to move with a velocity *v* in the x direction. Next to the upper plate, the liquid moves with the same velocity as the plate while the velocity of the liquid next to the lower plate is zero. A linear velocity gradient is assumed between the upper and the lower plate.

Viscosity is defined as the shear stress divided by the rate of deformation. The deformation (called *strain*) is defined as the angle of deformation resulting from a small displacement, Δx, of the upper plate in the x direction, i.e. $\theta = \arctan(\Delta x/d)$ where θ is the angle of deformation (Fig. 2). The symbol for strain is γ. The rate of deformation (i.e. *strain rate*, also called *shear rate*) is the magnitude of deformation per time unit (usually s^{-1}) in continuous shear, i.e. $d\gamma/dt$. The viscosity is therefore

$$\eta = \frac{\tau}{d\gamma/dt} = \frac{\tau}{\dot{\gamma}} \tag{1}$$

where η is viscosity (Pa·s) and $\dot{\gamma} = d\gamma/dt$ (s^{-1}).

Linear viscoelasticity

If a small strain deformation is applied on a solid material, the energy is in most cases stored elastically and upon removal of the strain deformation, the material reverts back to the original state. In other words, the net change in energy is zero (in practice there are always small energy losses in the form of structural changes, heat loss due to friction, etc.). Fluids usually exhibit both elastic and viscous character, hence the term ‘viscoelasticity’.
The most common way to quantify the viscoelastic character of a fluid is by measuring the response of a fluid sample to oscillatory shear at very small strain amplitudes. The theory behind linear viscoelasticity is based on the assumption that the response of the sample is directly proportional to the applied strain (or stress). If, for example, the applied strain is doubled, the stress response of the sample is also doubled. All coefficients of time differentials, e.g. viscosity, are not allowed to vary with changes in variables such as applied strain or strain rate. Thus, all differential equations are linear and easy to handle.

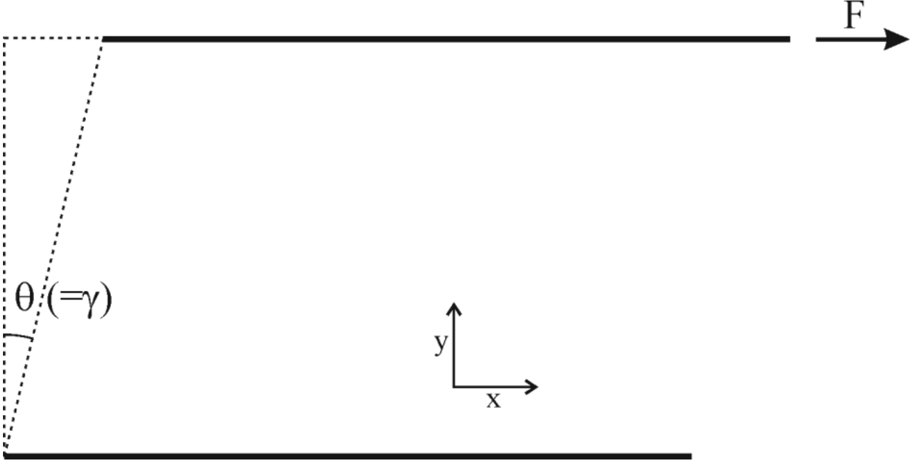

Figure 2. A force applied on a material results in deformation of the material. The resulting angle of deformation, θ, is defined as the strain, γ.

It is instructive to start by considering a static situation. A small stress applied on a solid material results in deformation (strain) of the material (Fig. 2). For as long as the applied stress persists, the deformation also remains. The *shear modulus* or *rigidity modulus* is defined as the ratio between stress and strain, i.e.

$$G = \frac{\tau}{\gamma} \tag{2}$$

where G is the shear modulus. It is also called rigidity modulus because in effect it is a 'coefficient of stiffness' for a material. Writing Eq. (2) in the form $\tau = G\gamma$, it is easy to see that the resulting stress in a material depends on the strain times a constant, G. An analogue can be found in Hooke's law of elasticity where the spring constant has the same significance as G has in Eq. (2).

In oscillatory shear the strain deformation takes place as a continuous movement both in the +x and –x direction (Fig. 2) at a certain amplitude and frequency. A frequency dependent *complex shear modulus*, G^*, is defined:

$$G^*(\omega) = \frac{\tau(t)}{\gamma(t)} \tag{3}$$

where τ and γ are now functions of time. If a sinusoidal oscillatory strain of amplitude γ_0 is applied on a material the strain will vary with time according to

$$\gamma(t) = \gamma_0 \exp(i\omega t) \tag{4}$$

where $i = \sqrt{-1}$ and ω is the angular frequency. The stress response, $\tau(t)$, of a perfectly elastic material is exactly in phase with the input strain, i.e. the phase angle, δ, between input strain and the stress response of the material is zero. For any material however, there is always a loss of energy and thus the stress response will be out of phase by an angle δ. A liquid usually exhibits both elastic response and viscous energy loss within a certain frequency range. This is called the viscoelastic region. Generally, at low frequencies mainly viscous loss is experienced and at high frequencies a larger portion of the energy is stored elastically.

Since the stress response of a material is assumed to be proportional to the input strain the stress varies with time according to

$$\tau(t) = \tau_0 \exp[i(\omega t + \delta)] \tag{5}$$

where τ_0 is the shear stress at γ_0. At constant amplitude and frequency G^* is only dependent on γ_0 and τ_0 and thus the time factor can be dropped from Eqs. (4) and (5). Combination of Eqs. (3)-(5) then yields

$$G^* = \frac{\tau_0}{\gamma_0}\exp(i\delta) = \frac{\tau_0}{\gamma_0}(\cos\delta + i\sin\delta) \tag{6}$$

Equation (6) is often written in the form

$$G^* = G' + iG'' \tag{7}$$

where $G' = (\tau_0/\gamma_0)\cos\delta$ and $G'' = (\tau_0/\gamma_0)\sin\delta$. G' is a measure of the energy stored in a cycle and is called the *elastic modulus* or *storage modulus*. G'' is a measure of the energy lost during a cycle and is called the *viscous modulus* or *loss modulus*. Equations (3)-(7) are strictly valid only in the linear viscoelastic region, where the sample response is independent of strain amplitude at constant frequency. This usually occurs at very small strain amplitudes.

Experimental

The materials and rheological methods used have been described elsewhere (Eriksson and Schatz 2015). Measurement data on some additional samples are presented in this work, but the methods used are the same as in (Eriksson and Schatz 2015). Optical Coherence Tomography (OCT) imaging was used to check the flow integrity of the sample in the rheometer in some cases. The OCT technique is described elsewhere (Lauri, Bykov and Myllylä 2011).

Shear sweeps

In general, montmorillonite suspensions up to solids contents of 1 vol % display very low shear viscosity and almost Newtonian behavior (see Figure 3). The only exception is sodium montmorillonite (NaMt) in 17 mM NaCl, that exhibits pronounced shear thinning over the range of investigated shear rates (Fig 3b).

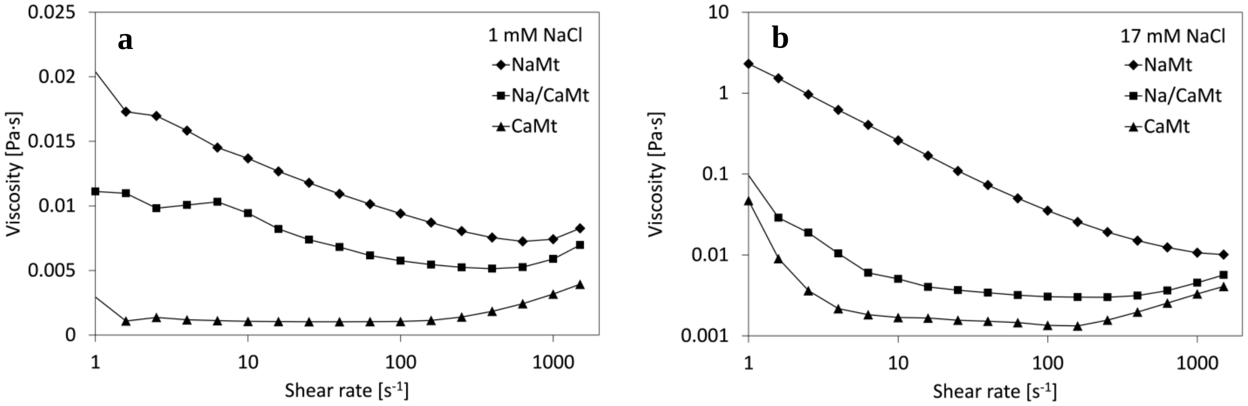

Figure 3. Shear viscosity of 1 vol % montmorillonite suspensions (with either Na or Ca as interlayer cation. See legend). The NaCl background electrolyte concentration is a) 1 mM and b) 17 mM.

A consistent trend in the shear viscosity curves is that NaMt suspensions have the highest viscosity and calcium montmorillonite (CaMt) suspensions have the lowest viscosity, while Na/CaMt fall in between (Fig. 3). This behavior is clearly related to the degree of flocculation (or more specifically, particle size), which has a two-fold effect on viscosity. First, an increased average particle size leads to increased sedimentation, which primarily affects the low shear rate viscosity (< ~10 s^{-1}) because at higher shear rates the particles are usually stirred into motion (depending on particle size). Second, at any given solids content, flocculation into larger particle aggregates leads to a reduction in the total number of particles in the suspension and consequently to a reduced number of collisions and therefore lower viscosity (Barnes, Hutton and Walters 1993). Both of these effects can be observed in Figure 1. NaMt particles are expected to exfoliate to some degree in aqueous suspension while CaMt particles are expected to remain as tactoids or aggregates in aqueous suspension, and this explains the observed differences in shear viscosity, both at low and high shear rates (Fig. 3).

A modest increase in electrolyte concentration (17 mM NaCl, Fig. 3b) leads to weakly networked structures in the suspensions, which is mainly observed as an increase in viscosity at low shear rates (< ~10 s^{-1}, Fig. 3b). As mentioned earlier, NaMt in 17 mM NaCl displays a much higher viscosity than any other montmorillonite suspension at the same solids content, and this indicates that the suspended solids arrange into volume-spanning structures that resist sedimentation at least over time-scales corresponding to the measurement duration (i.e. minutes). Moreover, the continuously decreasing viscosity (as opposed to NaCaMt and CaMt in Fig. 3b) indicates that any existing volume-spanning structure is broken down due to the applied shear but also that the remaining flocs lead to significant friction due to steric and/or electrostatic interactions. Any structures formed in Na/CaMt and CaMt suspensions in 17 mM NaCl on the other hand are quickly broken down by the applied shear (Fig. 3b) and above a shear rate of ~10 s^{-1} the viscosity stays constant and more or less identical to Na/CaMt and CaMt suspended in 1 mM NaCl (Fig. 3a).

Due to observations (via OCT imaging) of wall slip and shear banding at solids contents higher than 1 vol %, the measured viscosities where considered untrustworthy, and are therefore not reported.

Strain sweeps

The purpose of performing strain amplitude sweeps is usually to determine the linear viscoelastic region (LVR). The response of the sample is independent of the applied strain (and to some extent frequency) within the LVR and thus it is assumed that the macroscopic structure of the sample remains intact. At a certain strain amplitude, the response of the sample usually starts to vary with the applied strain (G’ decreases, G’’ often increases), and above this strain amplitude the sample structure cannot be considered to remain intact anymore.

A set of representative strain sweep measurements on montmorillonite suspensions are shown in Figure 4.

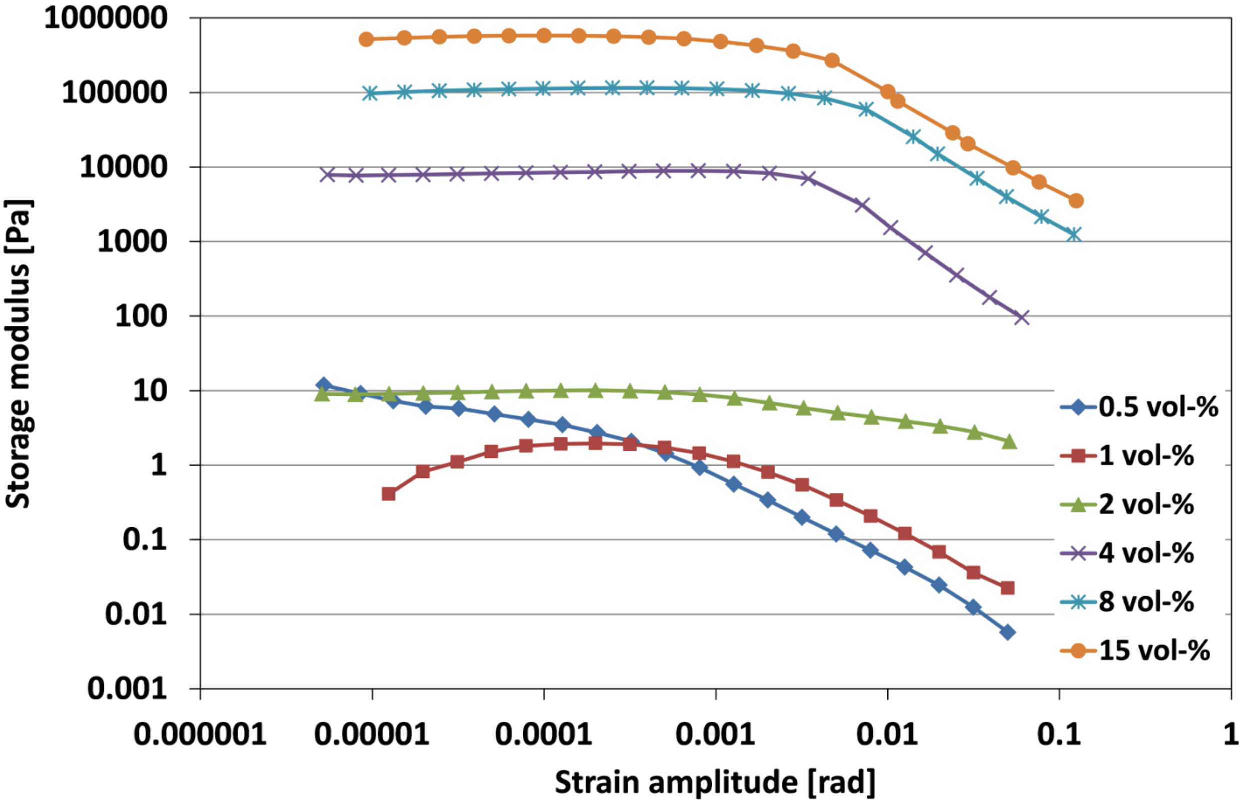

Figure 4. Strain sweep measurements on Na/CaMt suspensions in 1 mM NaCl at various solids contents. Only the storage modulus (G’) is shown. The frequency was 0.1 Hz in all measurements.

Practically all NaMt and Na/CaMt samples in 1 mM or 17 mM NaCl have strain sweep curves that are more or less similar in magnitude and shape as the curves shown in Figure 4 (at any given solids content). Below 4 vol % solids content there are differences in the shape of the G’ curve, but the order of magnitude of the measured storage modulus does not vary significantly between samples. Based on these results montmorillonite suspensions at solids contents ≤ 2 vol % can be considered liquid-like or phase separating (sedimenting). At ≥ 4 vol % solids content small variances in the measured storage modulus (in the LVR region) between different samples (at any given solids content) are within experimental error.

The LVR is easily identified for montmorillonite suspensions at solids contents ≥ 4 vol % as the strain amplitude range throughout which G' is constant and independent of the applied strain. Within this strain range the response of the sample is mostly elastic (phase angles vary between ~1 - 5°), and therefore the suspension structure can be regarded as remaining intact. It is interesting to note that the LVR upper strain amplitude limit (or failure strain, i.e. the strain amplitude at which G' starts to drop) occurs at approximately the same strain amplitude (~0.005 rad) for all samples in Fig. 4, regardless of solids content (at ≥ 4 vol %) or electrolyte concentration. Similar observations have been made elsewhere (Paineau, et al. 2011). The failure strain for the montmorillonite samples in Figure 4 (~0.005 rad) corresponds to a total oscillation displacement of ~60 µm, which translates into an effective oscillation displacement of ~30 µm (since the oscillation displacement occurs equally in the +x and –x directions, c.f. Fig. 2). In general, the failure strain is the same for all tested samples, except CaMt samples for which the failure strain occurs at slightly smaller amplitude. There are in fact indications that the failure strain is of the same order of magnitude over a wide range of solids contents. Resonant column tests (Fig. 5) (Pintado, et al. 2014) performed on highly compacted samples with water contents ranging between approximately 17 – 26 %, display failure strains of the same order of magnitude as the low solids content samples shown in Figure 4.

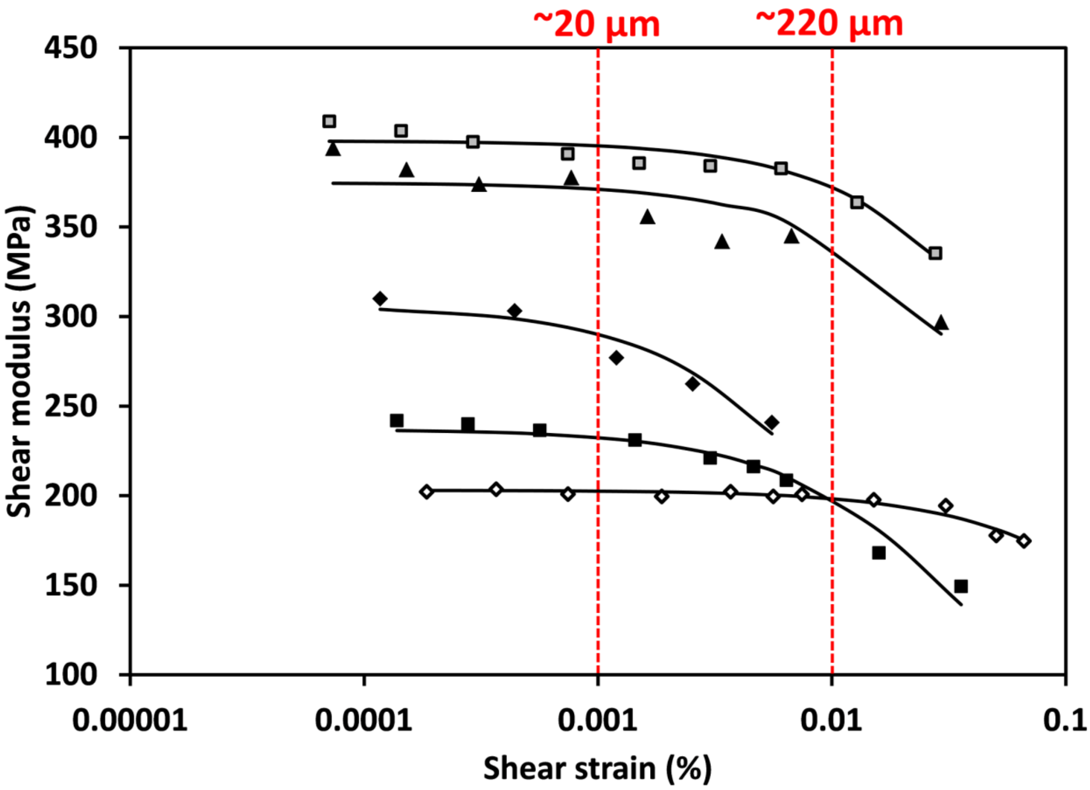

Figure 5. Shear modulus as a function of shear strain for compacted bentonite samples as determined by resonant column tests. The dry densities of the samples vary between 1.4 and 1.7 g/cm^3 and the water content varies between ~17 – 26 %. The solid lines are model calculations, see (Pintado, et al. 2014) for more information.

The failure strains for the compacted samples falls roughly in between the range marked by the red dashed lines in Figure 5. As indicated in Figure 5, this corresponds to effective oscillation displacements approximately between 20 – 220 µm, which is on average slightly larger than the oscillation displacement at the failure strain for the low solids content samples (Fig. 4). However, given the less well-defined range of constant shear moduli (comparable to the LVR in Fig. 4) in Figure 5 (as compared to Fig. 4) a reasonable approximation is that the failure strains are on the same order of magnitude in both cases.
The failure strain is closely linked to the macroscopic structure of the sample, which could involve structural properties such as some arbitrary repeating unit distance or aggregate size and/or bond flexibility. The failure strain amplitudes (tens of microns) measured in Figs. 4 and 5 are much larger than the size of a single clay platelet, or even a stack of several clay platelets arranged in parallel. It is therefore quite obvious that a suspension of homogeneously distributed clay platelets could not lead to a sample response such as seen in Figure 4 (at ≥ 4 vol % solids content). Instead, the magnitude of the failure strain indicates that domains of higher and lower density exist in these systems, at roughly the same length-scale as the effective failure strain (i.e. a few tens of microns). The domains of higher density must be clay aggregates, but the size of the aggregates or the nature of interactions between these aggregates cannot be unambiguously determined from strain sweep measurements.

The fact that the failure strain is on the same order of magnitude over a wide range of solids contents (possibly with a tendency to increase at higher solids contents or compaction levels) indicates that the mechanical properties of clay material is governed by either aggregate size or bond flexibility rather than some aggregate (or other feature's) repeating unit distance. The increasing LVR storage modulus (or shear modulus) as a function of solids content therefore reflects an increasing number of aggregates or bonds interacting with each other, while the maximum deformability (failure strain) of the material remains more or less constant.

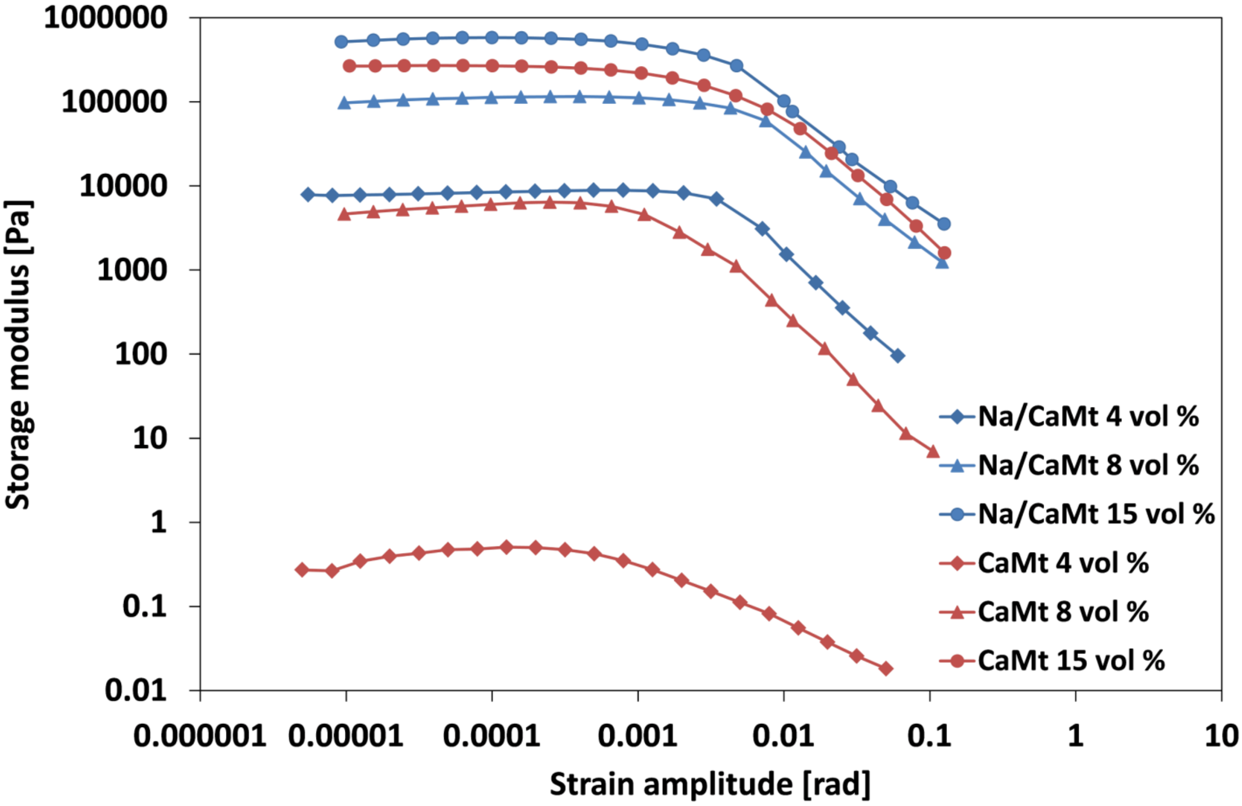

Figure 6. Strain sweep measurements performed on Na/CaMt and CaMt samples at various solids contents in 1 mM NaCl.

CaMt samples display consistently lower storage moduli (at any given solids content) than NaMt and Na/CaMt samples (see Figure 6). In addition, samples suspended in 170 mM NaCl generally have a lower storage modulus than samples suspended in low salinity water (not shown). The reason for the lower storage moduli in these cases is most likely sedimentation due to flocculation, even if the samples appear to be non-flowing and solid-like at the higher solids contents (≥ 8 vol %).

Frequency sweeps

Performing oscillatory shear at varying frequencies yields information about the time-dependent response of samples to a small strain deformation. A solid-like material will retain its structure in response to a small strain deformation (i.e. it responds elastically), while a liquid-like material will rearrange and relax its structure in response to a small deformation (i.e. it responds viscously), see Figure 7. For a viscoelastic material the response depends on frequency.

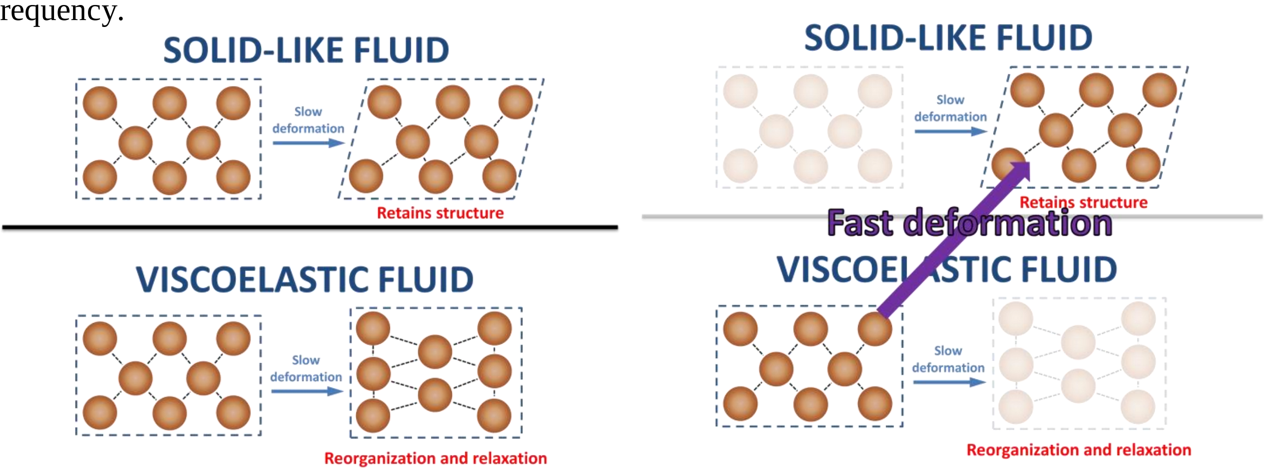

Figure 7. Schematic representation of the mechanical response of a solid-like fluid and a viscoelastic fluid to a small strain deformation. The brown spheres represent particles or aggregates and the dashed lines in between the spheres represent bonds of an arbitrary nature. A viscoelastic fluid will reorganize its structure and relax in response to a slow deformation (left panel), but in response to a fast deformation a viscoelastic fluid will retain its structure (right panel).

Frequency sweeps performed on 4 and 8 vol % montmorillonite samples are shown in Figure 8.

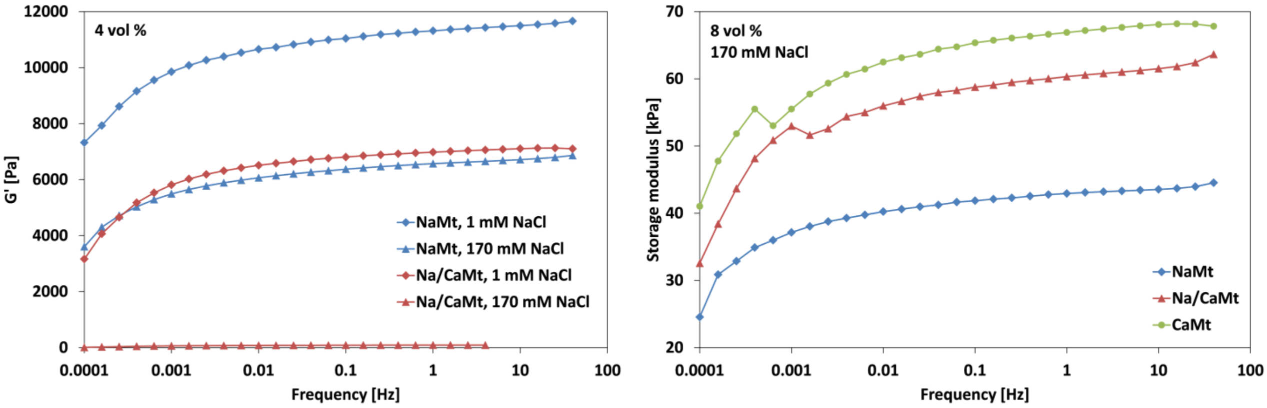

Figure 8. Frequency sweeps performed on 4 vol % (left) and 8 vol % (right) montmorillonite suspensions. The strain amplitude was ~0.5 mrad in all measurements.

A distinct decrease in storage modulus (G') is observed in all samples when going from high frequencies towards low frequencies. At high frequencies (> ~0.01 Hz) G' is fairly constant, but at lower frequencies (< ~0.01 Hz) G' starts to decrease considerably as a function of frequency, while simultaneously the phase angle starts to increase (not shown). This response is typical of a Maxwell-type viscoelastic material (Barnes, Hutton and Walters 1993). From a structural point of view, the bonds keeping the material (montmorillonite) intact respond very slowly to deformation, and if the deformation is fast, most of the bonds remain unbroken (as indicated in Fig. 7). As noted above, the storage modulus starts to decrease at an increasing rate below ~0.01 Hz, and on average, the total drop in storage modulus from the highest frequency to the lowest frequency is on the order of 40 % for all samples. This is a significant decrease in storage modulus and implies that substantial restructuring and relaxation occurs. Complete relaxation probably occurs at even lower frequencies (10^{-4} Hz is the lower limit of the instrument), and based on the results shown in Figure 8, the relaxation time for montmorillonite suspensions is on the order of several hours.

Assuming montmorillonite suspensions consist of aggregates and/or clusters of higher density domains, a small strain deformation would lead to friction between these domains. An OCT snapshot taken during an actual measurement gives an idea of the size and shape of these aggregates in dilute suspensions (Fig. 9).

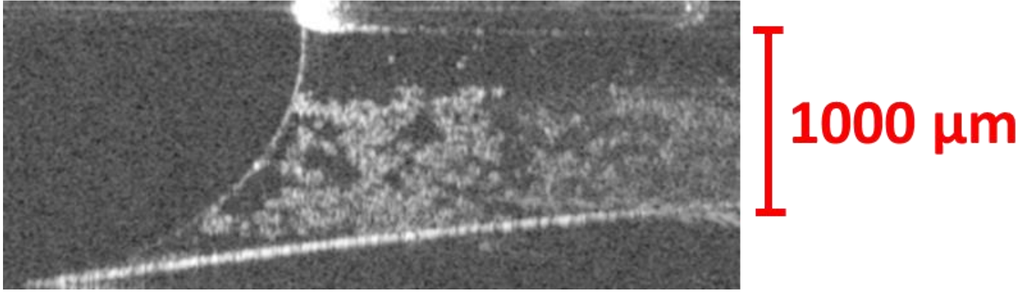

Figure 9. OCT image of 0.1 vol % NaMt in 17 mM NaCl during an actual rheological measurement. The gap between the plates is 1 mm. The lower plate appears to be curved but this is due to an optical distortion, and in reality it is perfectly flat. The white-colored areas between the plates consist of solid material (i.e. montmorillonite).

Based on the image shown in Figure 9, it seems that montmorillonite particles are able to form aggregates or clusters of considerable size (several tens of µm) even in very low solids content suspensions. At the solids content in Fig. 9 the aggregates necessarily have a very low density while, presumably, the aggregates are denser and perhaps smaller at higher solids contents. If the stress response of montmorillonite samples to a small deformation is due to friction between such aggregates (which seems likely), the relaxation process in a situation where the stress is upheld most likely involves deformation and restructuring of these aggregates. This could be a very slow process depending on the number of individual bonds that have to be broken and reformed. This process is further slowed down due to the irregular shape of montmorillonite flakes as compared to, for example, spherical particles. In any case, it appears that montmorillonite systems are dynamic (viscous) in nature rather than rigid, solid-like systems since they are able to relax in response to a very small applied strain.

Summary and considerations for geologic disposal

The rheological properties of a wide range of aqueous montmorillonite suspensions were studied. In general, a transition from liquid-like or phase separating behavior to viscoelastic behavior was found to occur between 2 – 4 vol % solids content. Earlier studies (Abend and Lagaly 2000) have indicated solid-like (or gel-like) behavior for montmorillonite suspensions at lower solids contents than 2 vol %, but in order to achieve this an external force (stirring, ultrasound etc.) has to be applied. From a practical point of view, the samples studied in this work were allowed to swell freely, and based on observations, 4 vol % was the minimum solids content at which non-sedimenting and homogeneous systems exhibiting viscoelastic behavior were formed. Since no measurements were conducted at solids contents between 2 and 4 vol %, it is possible that viscoelastic systems form below 4 vol % (but above 2 vol %) solids content.

Shear viscosities were determined for systems up to 1 vol % solids content, and it was found that most systems exhibit low viscosities (< 100 mPas) and nearly Newtonian behavior. With 17 mM NaCl as background electrolyte the low shear rate (< ~10 s^{-1}) viscosity was slightly increased as compared to 1 mM NaCl, which demonstrated the existence of weak structures in the systems. However, these structures were normally quickly broken down by the shear, and above shear rates of ~10 s^{-1} shear viscosities were generally very low (< ~15 mPas), and no significant differences were observed between the studied systems. The only system that behaved differently was NaMt suspended in 17 mM NaCl, which demonstrated a higher viscosity than all the other systems, and pronounced shear thinning. This implies that a weak volume-spanning structure exists in this system that resists sedimentation for at least the time it takes to perform a measurement (i.e. minutes).

Strain sweep and frequency sweep oscillatory shear measurements were performed on a wide range of samples at different solids content. In general, samples at solids content ≥ 4 vol % display a well-defined linear viscoelastic region (LVR), while samples below 4 vol % solids content cannot be considered to display a well-defined LVR. As expected, the magnitude of the storage modulus within the LVR increases as a function of solids content (at any given background electrolyte concentration). CaMt samples and NaMt or Na/CaMt samples suspended in 170 mM NaCl had significantly lower LVR storage moduli (at any given solids content) as compared to other samples, which suggests that sedimentation occurs, even at high solids content (> 4 vol %).

The failure strain in the strain sweep measurements occurred at the same strain amplitude for all samples, except CaMt samples for which the failure strain was, on average, slightly smaller. This implies that the macroscopic structure of montmorillonite suspensions does not change significantly as a function of solids content or electrolyte (NaCl) concentration. In fact, there are certain indications that the macroscopic structure of highly compacted samples is similar in length-scale as the macroscopic structure of dilute suspensions (4 – 15 vol %, see Figs. 4 and 5). The amplitude at the failure strain (corresponding to ~30 µm effective sample deformation) also suggests that the samples contain domains of higher densities (aggregates) and lower densities, i.e. they are not systems of homogeneously distributed particles. For a system consisting of homogeneously distributed particles the failure strain amplitude is expected to be smaller (on the order of a single (or a few) particle diameter(s)).

Frequency sweeps demonstrate that montmorillonite suspensions relax in response to a small applied strain over long time-scales (hours). These measurements confirm the true frequency dependent viscoelastic behavior of montmorillonite suspensions, and demonstrate that the structure can rearrange in response to a small applied strain. As such, montmorillonite suspensions should not be considered solid-like materials, but rather as viscoelastic liquids (at least within the solids content range investigated in this work) with a very high viscosity and possibly exhibiting a yield stress (Eriksson and Schatz 2015). Although a yield stress was determined for various montmorillonite samples (Eriksson and Schatz 2015), it was determined on the basis of oscillatory shear measurements at a certain frequency, and based on the results in Figure 8, it is clear that the calculated yield stress would have been different (lower) if the frequency would have been lower.

The most likely conditions under which dilute montmorillonite suspensions may occur in an underground repository is near locations where it is possible for buffer (or backfill) material to swell into an intersecting rock fracture. Artificial fracture tests have been used already for some time to study clay material extrusion into thin fractures, and it is clear that the extruding material has a solid-like appearance and consistency, and that a solids content gradient exists along the extruding material in a radial direction outwards from the center (high solids content near the center, low solids content at the extrusion front) (Schatz, et al. 2012). Based on the results presented in this study, the extruding clay material has a viscoelastic character with a long relaxation time (hours). In a previous study (Eriksson and Schatz 2015), it was determined that the yield stress of the material is most likely large enough to withstand mechanical shear caused by flowing groundwater, and therefore that possible erosive loss of clay material is purely due to chemical processes. However, at the time of the study by Eriksson and Schatz (2015), the viscoelastic nature of clay suspensions had not been fully determined, and as such some doubt still exists concerning the correctness of the calculated yield stress values (as noted above). This can easily be verified by additional rheological measurements though, and preliminary plans exist for conducting these measurements.
As a final note, the data presented in this work has yielded a lot of information on the mechanical properties of dilute clay suspensions and therefore it is suggested that related modeling efforts take advantage of that.

References

Abend, S., and G. Lagaly. “Sol-gel transistions of sodium montmorillonite dispersions.” *Applied Clay Science* 16 (2000): 201-227.

Barnes, H. A., J. F. Hutton, and K. Walters. *An Introduction to Rheology.* 3rd. Amsterdam: Elsevier Science Publishers B.V., 1993.

Eriksson, R., and T. Schatz. "Rheological properties of clay material at the solid/solution interface formed under quasi-free swelling conditions." *Applied Clay Science* 108 (2015): 12-18.

Lauri, J., A. V. Bykov, and R. Myllylä. "Determination of suspension viscosity from the flow velocity profile measured by Doppler optical coherence tomography." *Photonics Letters of Poland* 3, no. 2 (2011): 82-84.

Paineau, E., L. J. Michot, I. Bihannic, and C. Baravian. "Aqueous suspensions of natural swelling clay minerals 2. Rheological characterization." *Langmuir* 27 (2011): 7806-7819.

Pintado, X., E. Romero, J. Suriol, and A. Lloret. *Small-strain stiffness of statically compacted MX-80 bentonite using resonant column tests.* TM 29/237, Helsinki: B+Tech Oy, 2014.

Schatz, T., N. Kanerva, J. Martikainen, P. Sane, M. Seppälä, A. Olin, and K. Koskinen. *Buffer erosion in dilute groundwater.* Posiva Report 2012-44, Olkiluoto: Posiva Oy, 2012.